April 26, 2006
version 0.1

MC Validation Using $Z^0 + 1$ Parton Sample

Yoshio Ishizawa (TRIUMF)
yoshio@triumf.ca

Abstract

This note describes a Monte Calro validation study using Z^0+1 parton samples. The $Z^0 + 1$ parton events are privately generated using PYTHIA, then simulated by ATLAS full simulation in Athena v11.0.41. To validate the MC sample, some basic kinematic plots are made using Analysis Object Data (AOD) and the EventView package, and some funny behavior is found for muon E, missing energy and jet η, and jet energy resolution which will require for the investigation.

1 Introduction

$Z^0 + 1$ jet is a good sample for jet energy scale studies, since the p_T of the Z^0 and jet are expected to be equal and opposite. To do the jet energy scale studies correctly, it is important to validate the MC sample. This document describes the $Z^0 + 1$ parton MC sample validation for electrons, muons, missing energy, and jets. The $Z^0 + 1$ parton events are generated using PYTHIA with parton $p_T > 3$ GeV/c or $p_T > 50$ GeV/c, then simulated using ATLAS full simulation in Athana v11.0.41, where Z^0 boson decays to electrons or muons only. Table 1 shows the number of events generated with each p_T cut. All events are reconstructed to form Analysis Object Data (AOD), and the EventView package with default job options (The cone radius (R) for jet reconstruction is changed from $R = 0.5$ to $R = 0.4$) is used in this analysis to resolve overlaps between different particle types within the AOD. The analysis is also based on comparisons between measured and generated objects. The generated objects are retrieved from the "SpclMC" container.

Parton p_T	Events
$p_T > 3$ GeV/c	143,122
$p_T > 50$ GeV/c	39,336
Total	182,458

Table 1: $Z^0 + 1$ parton MC samples

2 Validation

2.1 Electron

To compare generated electrons with measured electrons, the closest generator level electrons to the measured electrons are used using $dR = \sqrt{d\eta^2 + d\phi^2}$, where $d\eta$ and $d\phi$ denote the angles between measured and generated electrons in $\eta - \phi$ space. Figure 1 shows E_T, η and ϕ distributions for the measured and generated electrons, and the E_T correlation. Electrons are well reconstructed.

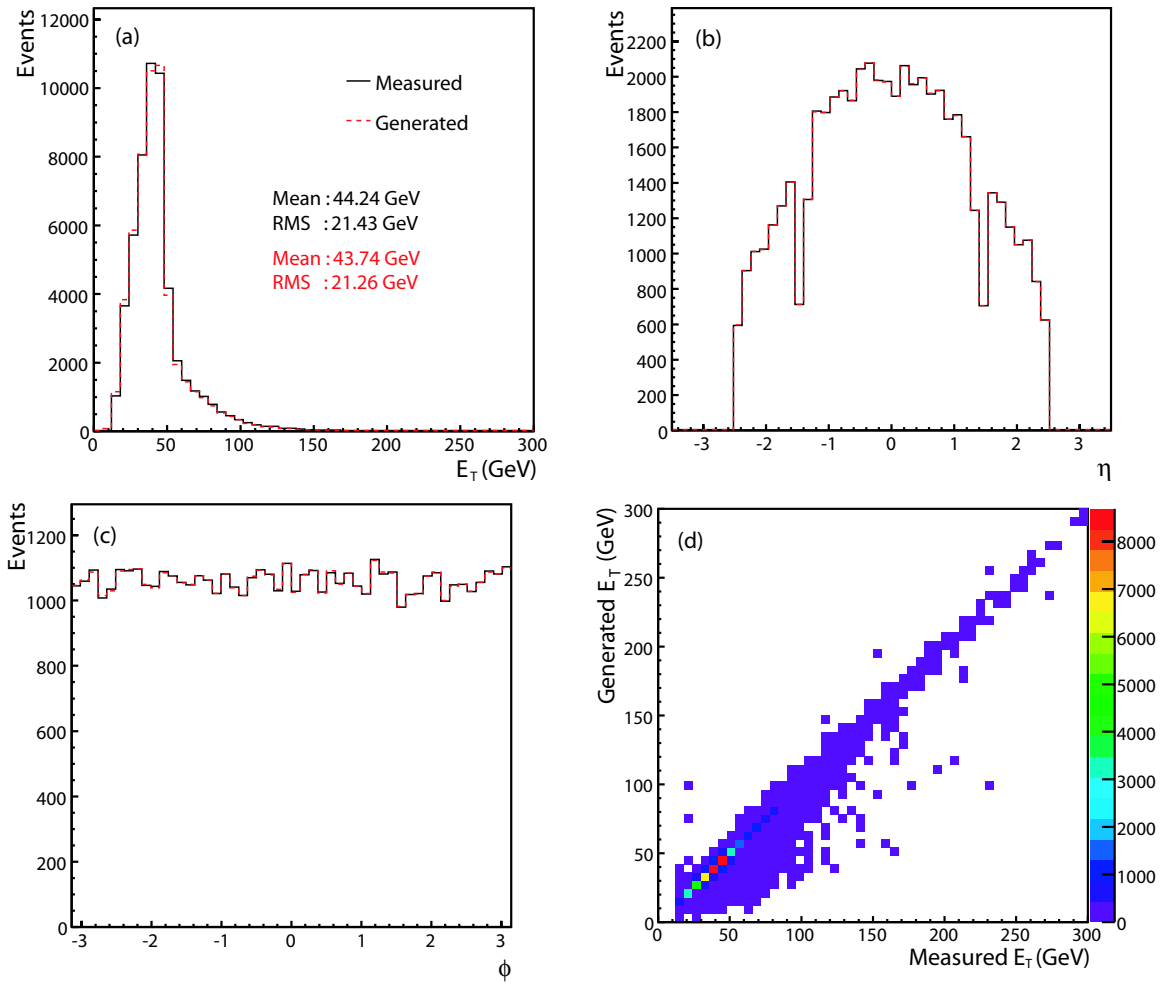

Figure 1: (a)E_T, (b)η and (c)ϕ distributions for the measured and generated electrons, and (d)E_T correlation.

2.2 Muon

For the muon comparison, the same dR matching as for electrons is used. Figure 2 shows the p_T, η and ϕ distributions for the measured and generated muons, and the p_T correlation. Figure 3 shows E and p distributions, and the correlations. Although muon momenta are well reconstructed, some measured muons have larger energies than generated. Figure 4 and

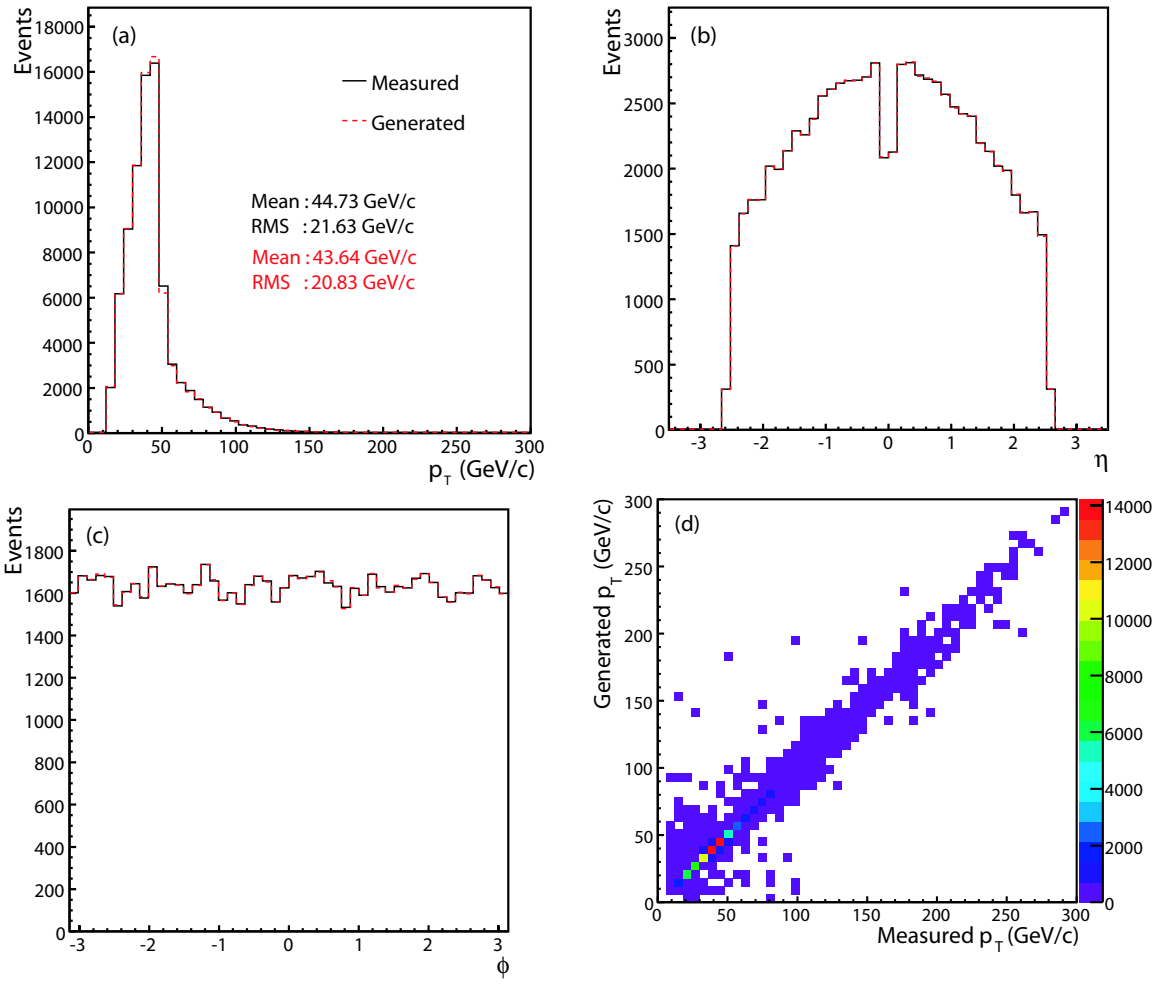

Figure 2: (a)p_T, (b)η and (c)ϕ distributions for the measured and generated muons, and (d)p_T correlation.

Figure 5 show correlations between E and p for the measured and generated muons, and the ratio for the measured muons. Some measured muon energies are not well reconstructed, and the measured muons are reconstructed with 1.4 times as large as generated muon energies.

2.3 Z^0 Boson

Z^0 bosons are reconstructed using di-lepton events with opposite charges. Figure 6 shows the reconstructed Z^0 mass distributions. The mass distributions are fitted by Breit-Wigner functions. The Z^0 mass for the electron channel is well reconstructed, with a width of 4.7 GeV/c^2. However, the Z^0 mass distribution for muon channel has higher mass tail, because some muons are reconstructed with larger energies than generated, as described in Sec. 2.2. For the mis-reconstructed muons, $E/p > 1.2$ cut is applied (See Figure 5). Figure 7 shows the Z^0 mass distribution after removing events with the mis-reconstructed muons. There is no high mass tail in the mass distribution.

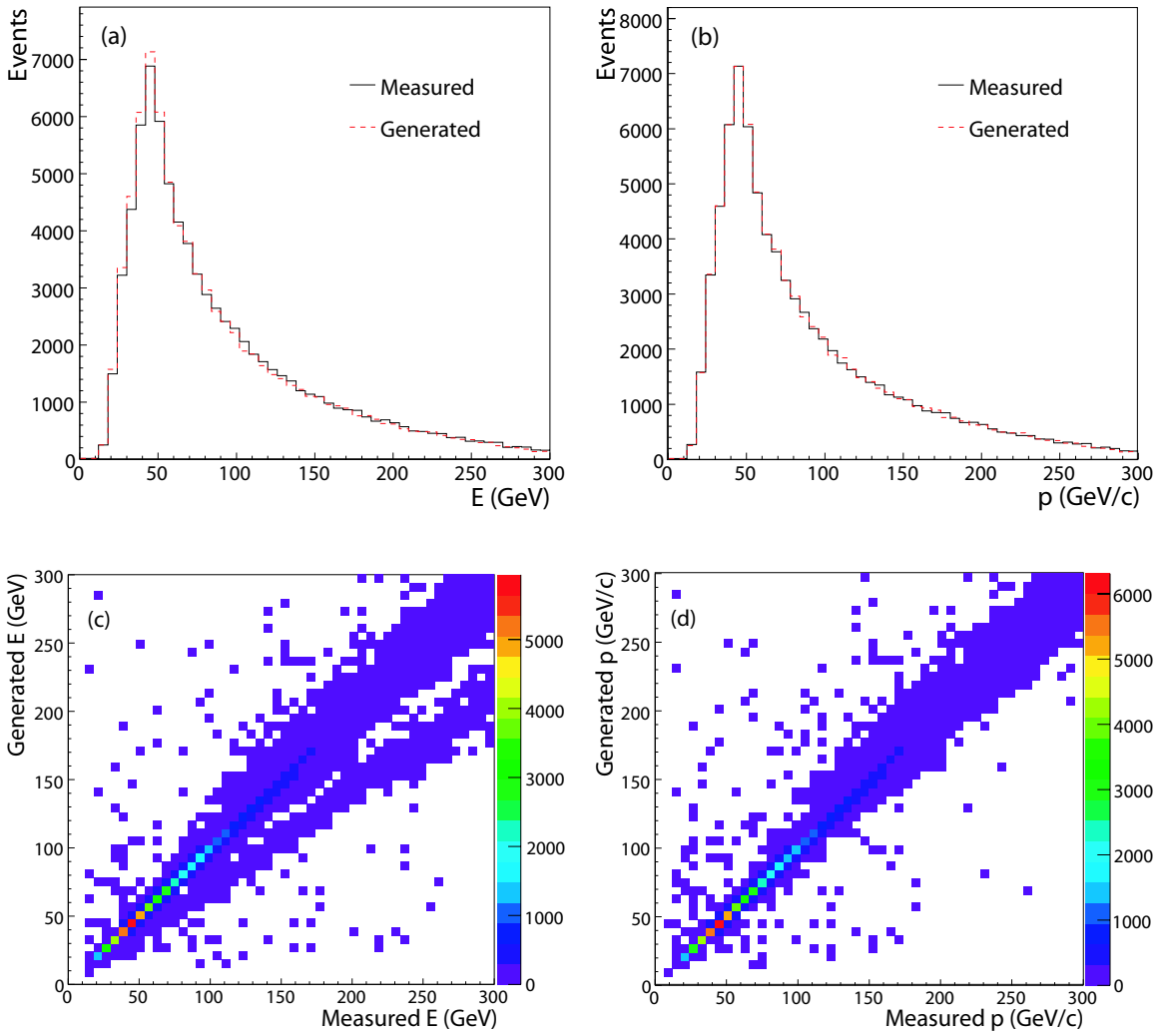

Figure 3: (a)E, (b)p, (c)E correlation and (d)p correlation for muons.

2.4 Missing Energy After $Z^0(\to \ell\ell)$ Requirement

Figure 8 shows the missing E_T, E_x and E_y distributions after $Z^0(\to \ell\ell)$ requirement. Since muons escape from detectors with large momentum, the corrections for muon p_T are applied to the missing energies. However, there are a peak and tails for $Z^0 \to \mu^+\mu^{-1}$. For muon channel, a event selection to remove events with the mis-reconstructed muons using $E/p > 1.2$ is also applied, but these peak and tails remain.

2.5 Jet

Jets are reconstructed cone algorithm with $R = 0.4$. Figure 9 shows multiplicity, E_T, η and ϕ distributions for the measured jets. For η distribution, there are peaks around $|\eta| = 0.0$ and $|\eta| = 1.5$.

[1]Although the muon spectrometer does not cover $\eta = 0$, the effects are ignored, because the plots are made after the $Z^0(\to \mu^+\mu^-)$ requirement.

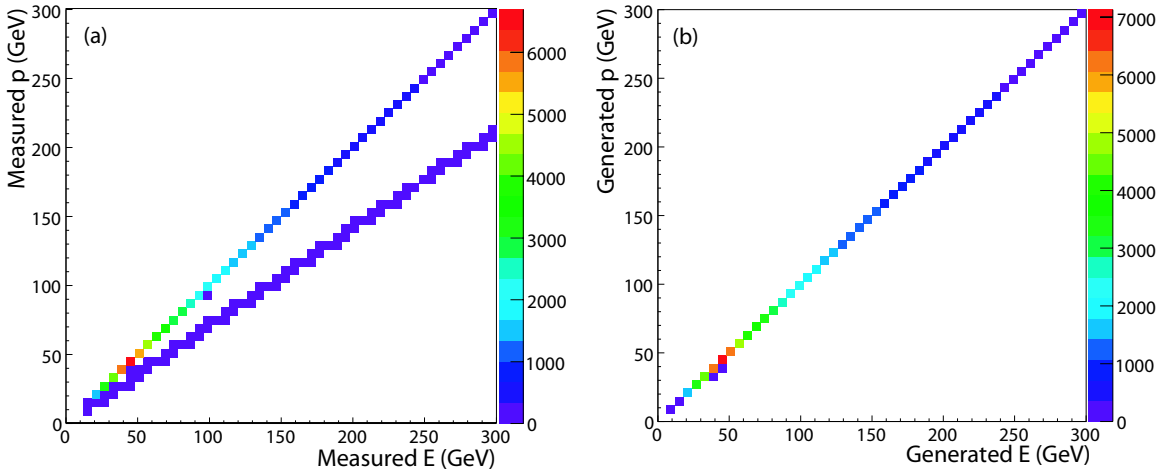

Figure 4: Correlations between E and p for muons. (a)measured muons, (b)generated muons.

2.5.1 Jet E_T Comparison

To compare generator level parton E_T with the measured jets, events reconstructed with one jet are required; Z^0 boson reconstruction is not required, to increase statistics. Then the parton-jet matching is required with $dR = \sqrt{d\eta^2 + d\phi^2} < 0.4$ and generated parton $E_T > 15$ GeV[2]. Figure 10 shows efficiencies for the parton-jet matching. Since at low E_T jet reconstruction is more difficult, the efficiencies for low E_T jets are lower than those for high E_T jets. The efficiencies are also lower around $|\eta| \sim 1.5$, because of calorimeter cracks.

Figure 11 shows jet E_T distributions after the parton-jet matching for $0 < |\eta| < 1$, where the generated parton E_T ($E_T^{\rm Gen}$) is split into the following regions:

1. $15 < E_T^{\rm Gen}$ (GeV)< 25,
2. $25 < E_T^{\rm Gen}$ (GeV)< 35,
3. $35 < E_T^{\rm Gen}$ (GeV)< 50,
4. $50 < E_T^{\rm Gen}$ (GeV)< 80,
5. $80 < E_T^{\rm Gen}$ (GeV)< 120,
6. $120 < E_T^{\rm Gen}$ (GeV).

Figure 12 shows jet E_T ratio defined by $E_T^{\rm Meas}/E_T^{\rm Gen}$, where $E_T^{\rm Meas}$ is the measured jet E_T. The measured jets at low E_T are reconstructed with up to 20% higher energies than generated. The measured jets at high E_T are well reconstructed.

2.5.2 Jet Energy Resolution

Jet energy resolutions are also calculated from Gaussian fit parameters. The jet energy resolution is defined by σ_{E_T}/E_T at the $E_T^{\rm Gen}$ range, where the E_T and σ_{E_T} are Gaussian

[2]Jet E_T threshold is 15 GeV.

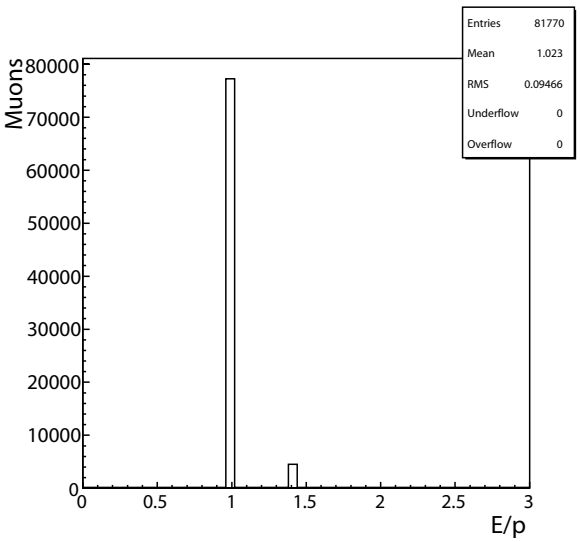

Figure 5: The ratio of E to p for the measured muons.

η region	$\sigma_{\text{stochastic}}$	σ_{constant}
$0 < \|\eta\| < 1$	1.21 ± 0.07	0.13 ± 0.01
$1 < \|\eta\| < 2$	1.12 ± 0.08	0.12 ± 0.01
$2 < \|\eta\| < 3$	0.67 ± 0.11	0.14 ± 0.01

Table 2: The fit results for jet energy resolution.

central value and width. Also, mean of the histogram for the generated partons is used as the representative point in the E_T^{Gen} ranges (the error is defined by R.M.S./$\sqrt{N}$, where R.M.S. and N are the root-mean-square and entries in the histogram for the generated partons). Figure 13 shows the resolutions for $0 < |\eta| < 3$, then the resolutions are fitted by

$$\frac{\sigma_{E_T}}{E_T} = \frac{\sigma_{\text{stochastic}}}{\sqrt{E_T}} \oplus \sigma_{\text{constant}},$$

where $\oplus$ means $A \oplus B = \sqrt{A^2 + B^2}$. Table 2 shows the fit results. For central calorimeters, the resolutions seems to be worse than expected.

3 Conclusion

The validation of $Z^0 + 1$ parton MC samples is conducted using AOD and the EventView package in Athena v11.0.41.

- Some muons are reconstructed with 1.4 times as large as the generated muon energies,
- Missing energy distributions have an additional peak and tails for $Z^0 \to \mu^+\mu^-$,
- Jet η distribution has peaks around $\eta = 0.0$ and 1.5,
- Jet energy resolutions seem to be worse than expected.

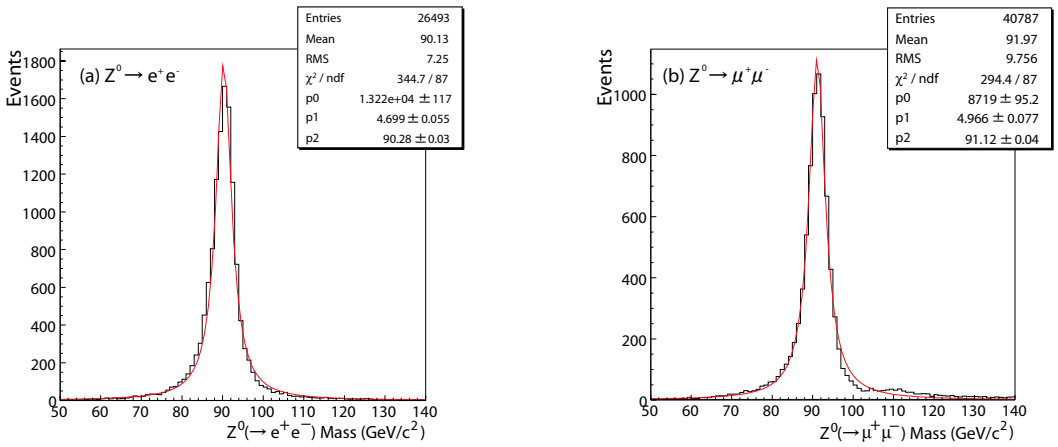

Figure 6: The reconstructed Z^0 mass distributions from di-lepton events with opposite charges. (a)$Z^0 \to e^+e^-$, (b)$Z^0 \to \mu^+\mu^-$.

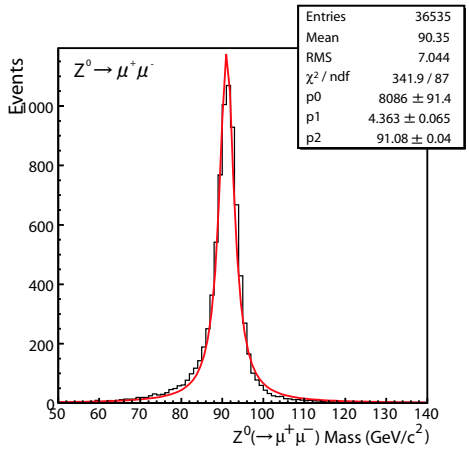

Figure 7: The reconstructed Z^0 mass distribution for $Z^0 \to \mu^+\mu^-$ after removing events with mis-reconstructed muons.

These problems should be investigated before starting to study jet energy scale and missing E_T.

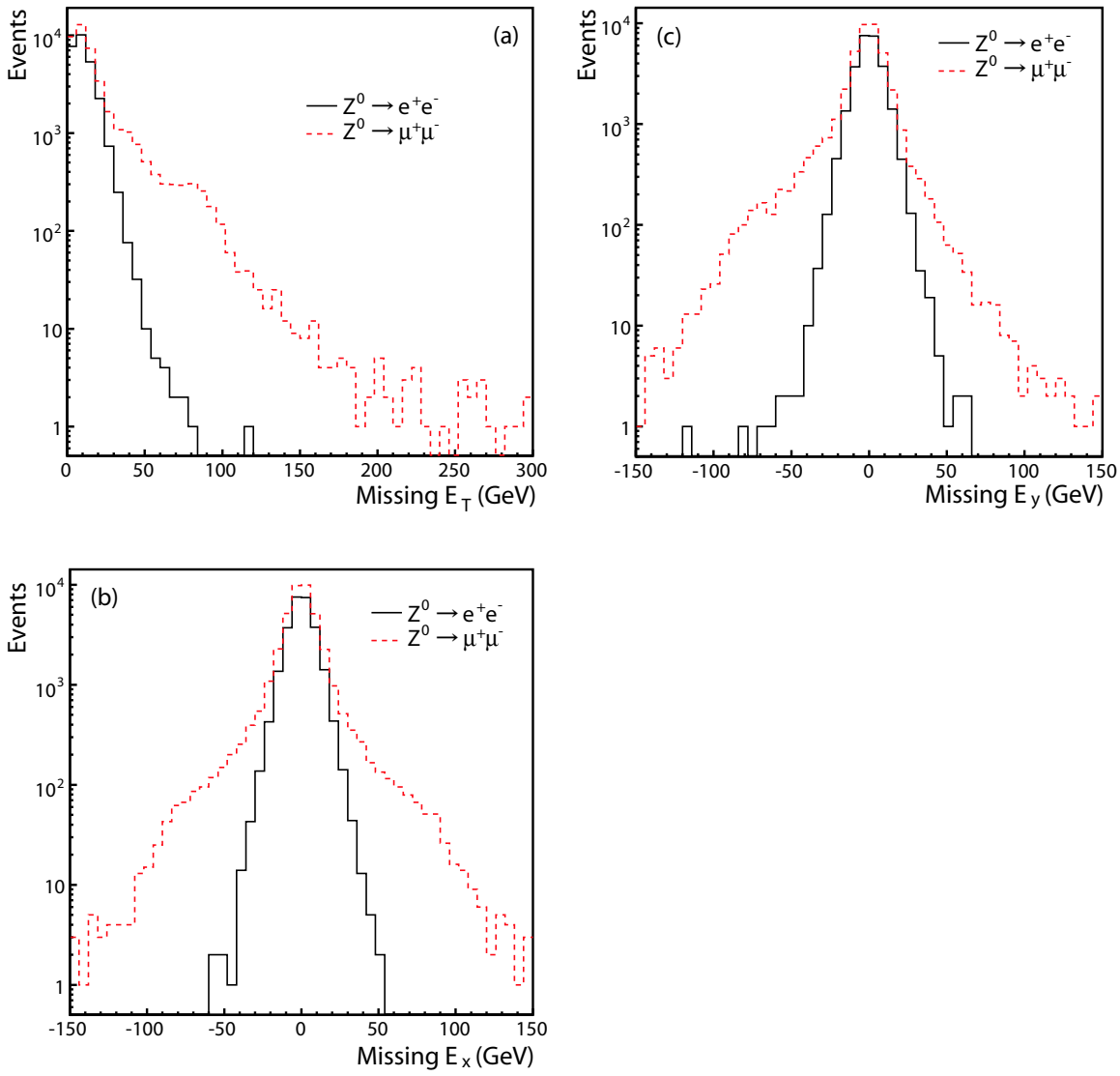

Figure 8: Missing energy distributions. (a)Missing E_T, (b)Missing E_x and (c)Missing E_y.

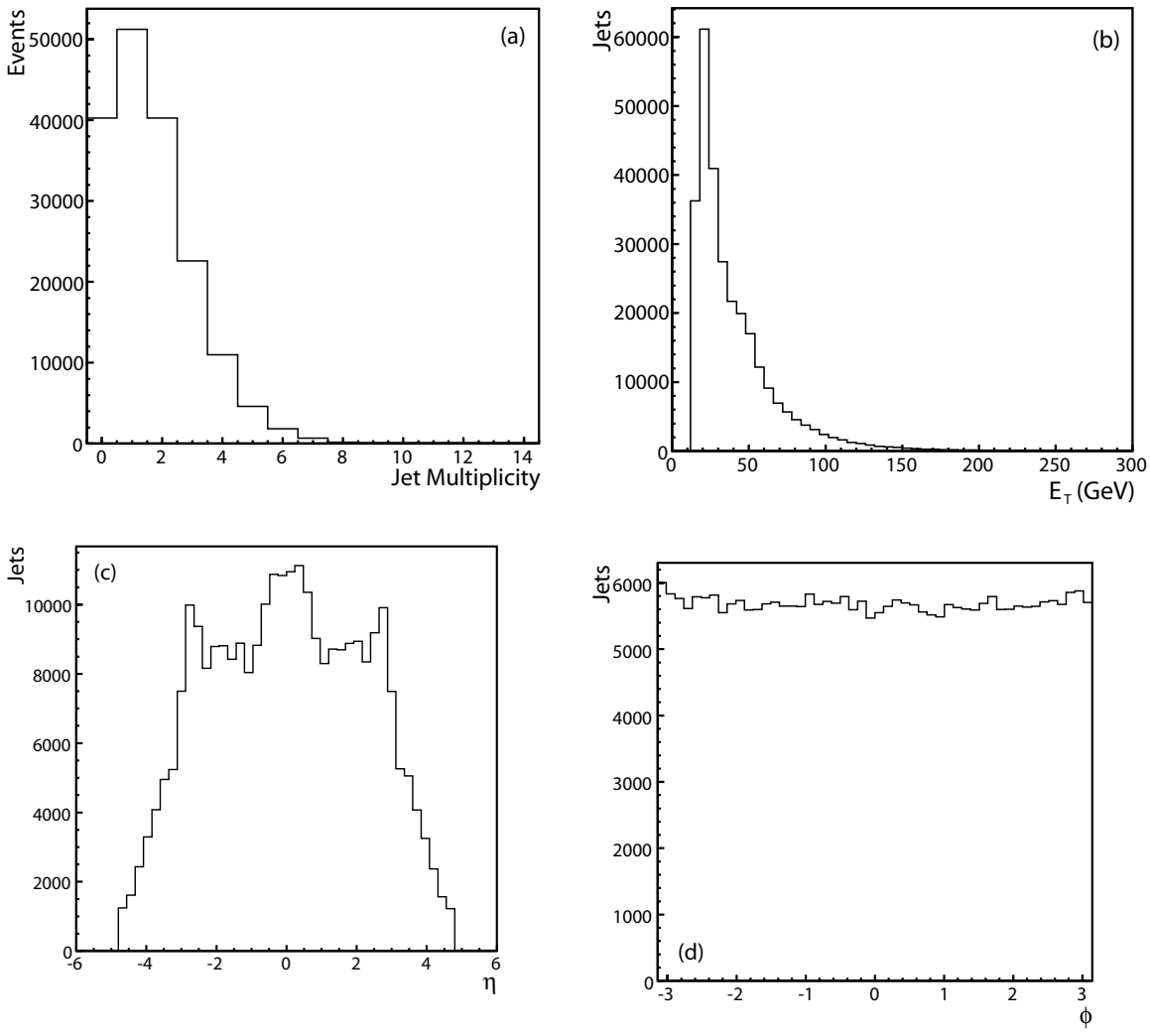

Figure 9: (a)Jet Multiplicity, (b)E_T, (c)η and (d)ϕ distributions for the measured jets.

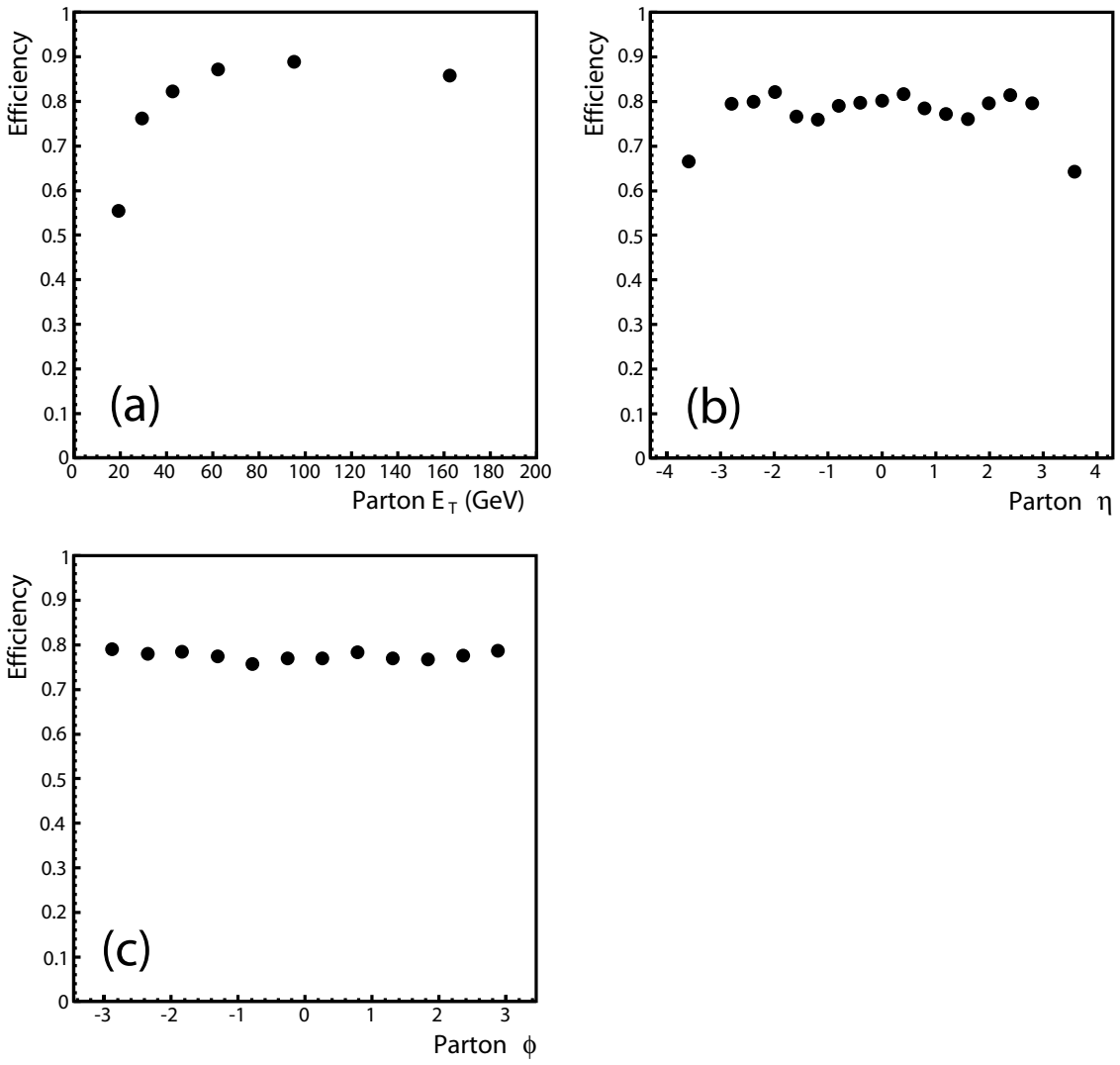

Figure 10: Efficiencies for the parton-jet matching as a function of the generated parton (a) E_T, (b)η, and (c)ϕ.

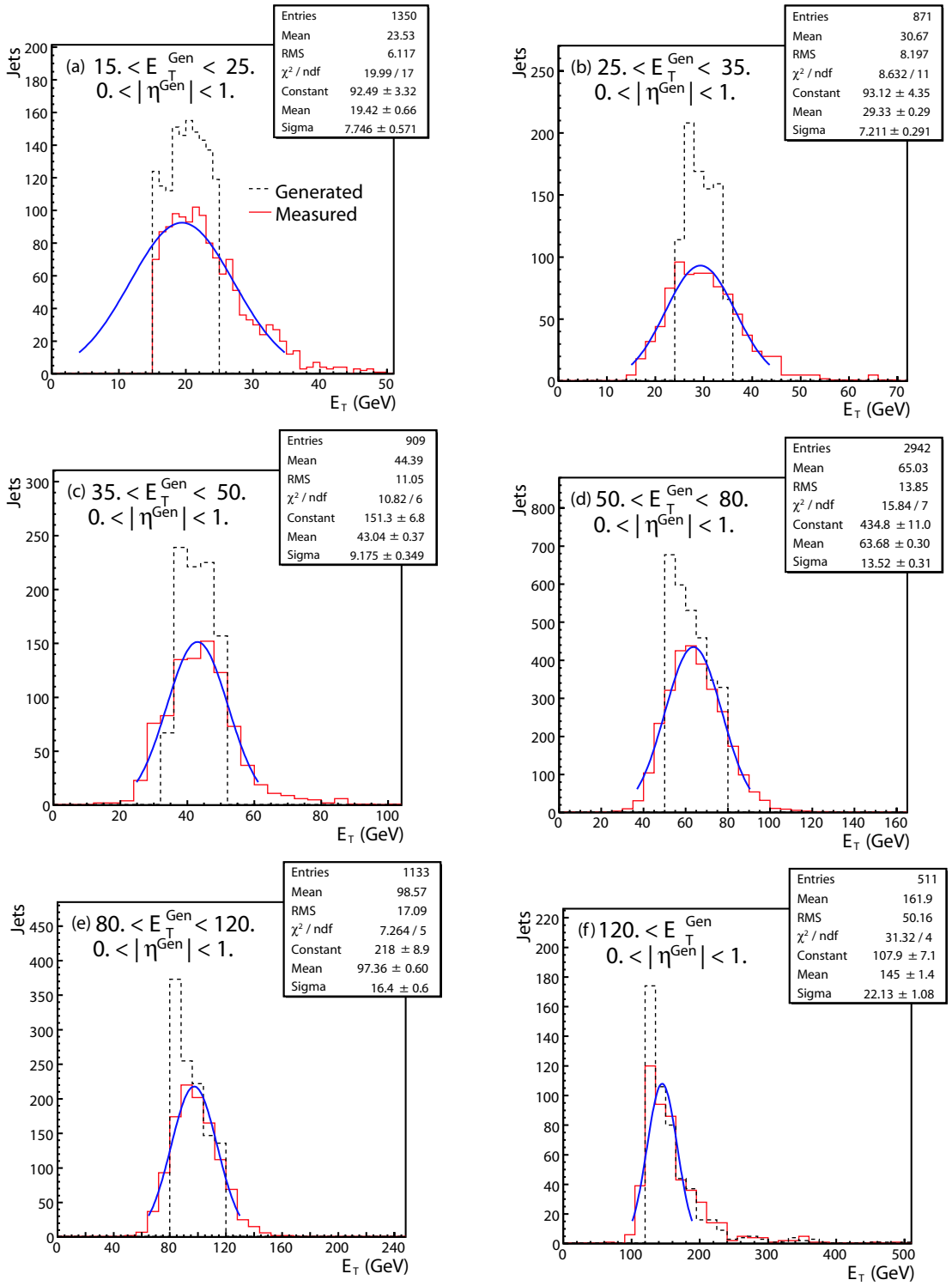

Figure 11: Jet E_T distributions for $0 < |\eta| < 1$. (a)$15 < E_T^{\rm Gen}$ (GeV)< 25, (b)$25 < E_T^{\rm Gen}$ (GeV)< 35, (c)$35 < E_T^{\rm Gen}$ (GeV)< 50, (d)$50 < E_T^{\rm Gen}$ (GeV)< 80, (e)$80 < E_T^{\rm Gen}$ (GeV)< 120, (f)$120 < E_T^{\rm Gen}$ (GeV), where $E_T^{\rm Gen}$ denotes the generated parton E_T.

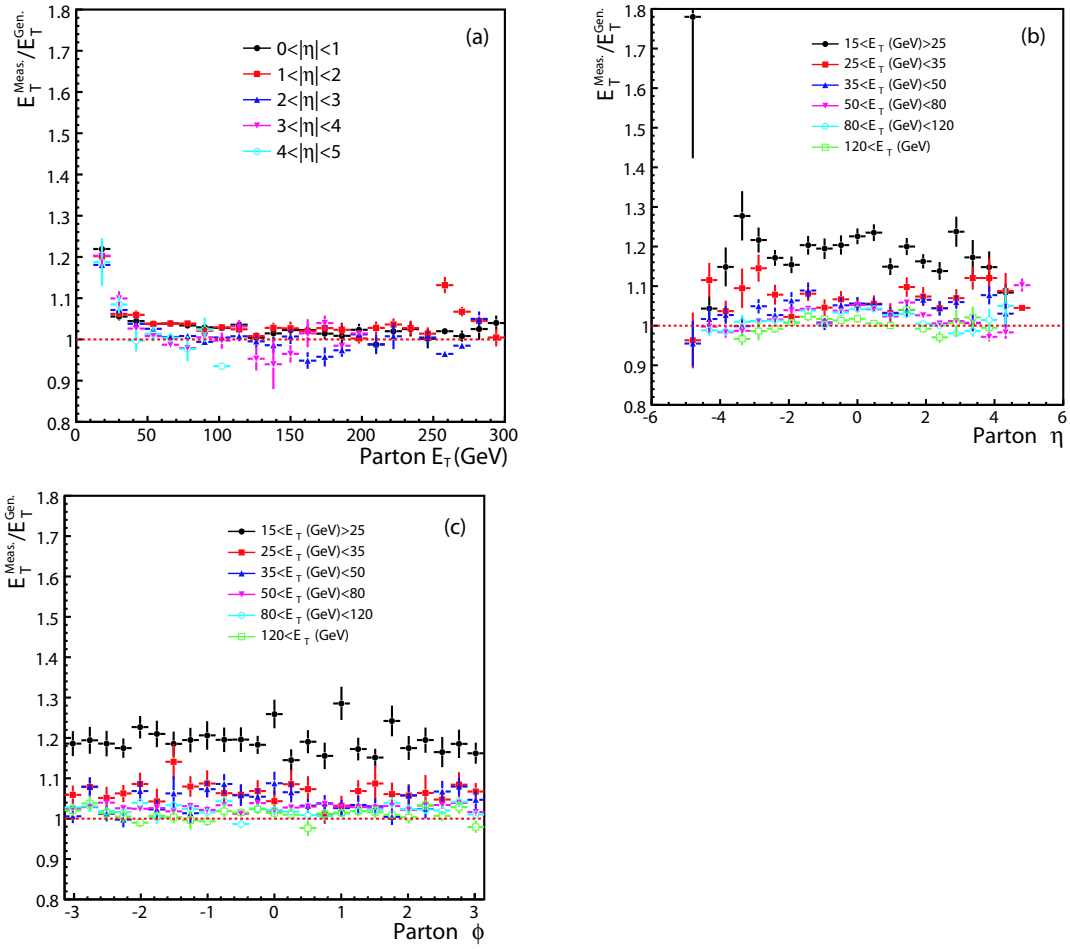

Figure 12: Jet E_T ratios as a function of parton (a)E_T, (b)η and (c)ϕ.

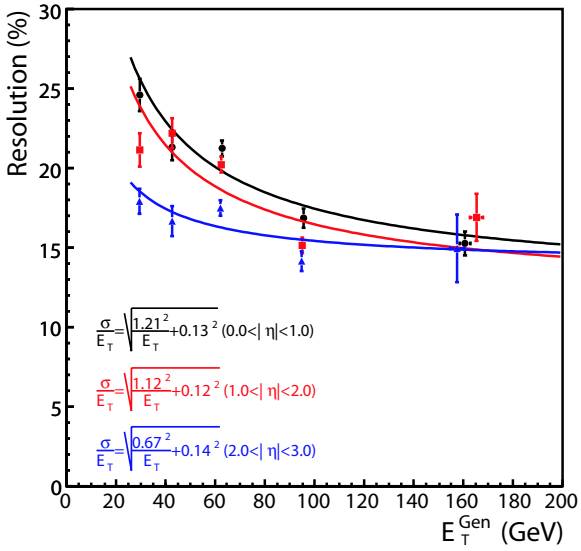

Figure 13: Jet energy resolutions as a function of the generated parton E_T.